DOI 10.1007/s11182-015-0570-1

Russian Physics Journal, Vol. 58, No. 6, October, 2015 (Russian Original No. 6, June, 2015)

ESTIMATION OF FRACTURE TOUGHNESS OF SMALL-SIZED ULTRAFINE-GRAINED SPECIMENS

E. E. Deryugin and B. I. Suvorov

UDC 624.014

*The results obtained from measurements of the crack resistance of a VT6 alloy (*Ti–6.46Al–3.84V *in wt.%) produced by refining coarse-crystalline structure down to an ultrafine-grained state, using a triaxial forging technique, are presented. The specific fracture energy γ_c is calculated by means of a new procedure developed for small-sized chevron-notched specimens. Severe plastic deformation is shown to cause a substantial reduction in γ_c at room temperature. Fracture surface structure found in the ultrafine-grained alloy under study contains local zones of a severely deformed material characterized by high pore concentration. This type of structure cannot be formed solely by crystallographic shearing along densely packed lattice planes. This is evidence for a significant role of rotation deformation modes in crack nucleation and growth on different structural scales of the material.*

Keywords: ultrafine-grained structure, localization of deformation, fracture, specific fracture energy, titanium alloys.

INTRODUCTION

Standard crack resistance tests typically involve massive specimens no less than 10 mm in thickness [1]. However, there is a practical need for conducting this kind of tests with the use of substantially smaller specimens. This is a vital issue for ultrafine-grained (UFG) and nanocrystalline materials produced by severe plastic deformation (SPD) techniques. The materials are characterized by fairly uniform crystallite size and misorientations in blanks of relatively low thickness. Besides, a tendency towards miniaturization of products in the most important branches of modern industry calls for estimation of crack resistance using techniques different from traditional approaches. An advantage of small-sized specimens is the fact that their testing does not require large amounts of materials and powerful testing machines. In fracture toughness (crack resistance) tests on small-sized samples, use is generally made of chevron-notched specimens [2–5]. There is no need to provide fatigue precracking in this specimen configuration.

The main parameter characterizing the ability of materials to resist crack growth is the critical stress intensity factor K_{Ic} to be usually calculated. The latter describes a non-uniform stress field in the vicinity of a crack tip in quasi-brittle materials. In metals and alloys, crack nucleation and growth are preceded by considerable plastic deformations. Calculations performed in [6] by the relaxation element method showed that the stress distribution in a plastic deformation zone differed essentially from the stress field in a cracked elastic medium. This is due to the fact that there is no singularity in this zone. As the distance from the crack tip increases, the stress increases from zero at the crack tip, passes through a maximum, and decreases gradually down to the level of the applied stress at a fairly great distance from the crack tip. This implies that K_{Ic} has no physical meaning for plastic materials, especially in the case of small-sized specimens.

Whatever the type of the material, a reliable characteristic of the crack resistance is the critical elastic energy release rate G_{cr} in crack growth. Notably, G_{cr} is equivalent to the value of the J-integral [7 and 8]. Using a new

Institute of Strength Physics and Materials Science of the Siberian Branch of the Russian Academy of Sciences, Tomsk, Russia, e-mail: dee@ispms.tsc.ru. Translated from Izvestiya Vysshikh Uchebnykh Zavedenii, Fizika, No. 6, pp. 47–51, June, 2015. Original article submitted March 6, 2015.

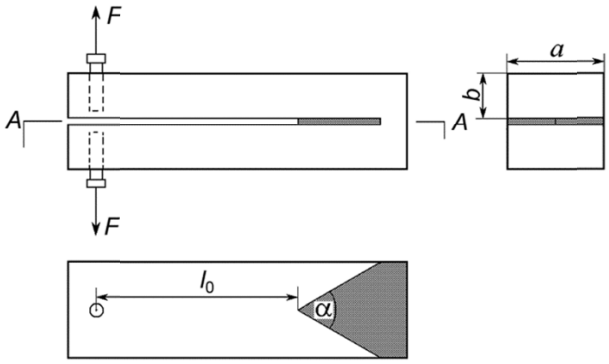

Fig. 1. Schematic representation of a chevron-notched specimen.

procedure developed in Laboratory of Physical Mesomechanics and Non-Destructive Testing Methods at Institute of Strength Physics and Materials Science of the Siberian Branch of the Russian Academy of Sciences (Tomsk, Russia), we have estimated the fracture toughness (crack resistance) of a VT6 alloy (Ti-6.46Al-3.84V) in initial coarse-crystalline (CC) and UFG states produced by the triaxial forging technique. Computations were performed taking into account chevron notch geometry, and the specific fracture energy was calculated. The findings of the investigations are discussed in the context of a multiscale approach of physical mesomechanics.

EXPERIMENTAL PROCEDURE

The test material was an UFG Ti-6.46Al-3.84V alloy (the grain size was 400 nm) produced by triaxial forging of a blank with a stepwise lowering of temperature in the range 1073–823 K. Each temperature stage involved multiple 50 % reduction operations with a change in the deformation axis of the blank [9]. We have also tested specimens of the alloy in the initial CC state with an average grain size of 8–10 μm.

A PENTAX K-5 camera was used every 3 s to obtain images of the lateral surface of a deformed specimen from which the crack length and crack tip opening were measured in the chevron notch zone. The surface fractographic patterns were examined by scanning electron microscopy (SEM). The specimens were subjected to room-temperature loading at a velocity of $\upsilon = 5$ μm/s by inserting a wedge with an angle of $\alpha' = 20°$ in the notch. A 28 mm long specimen was cut from rods of 6 × 6 mm^2 cross section. A chevron notch in the form of a (0.25 ± 0.05) mm wide slot dividing the specimen thickness in two equal parts was cut by the electroerosion technique. The notch boundary was set as a V-shaped line, with notch angle $\alpha = \pi/3$ (Fig. 1).

ESTIMATION OF THE SPECIFIC FRACTURE ENERGY

The necessary condition for the onset of crack growth in a flat specimen of unit thickness obeys the following equation [7–9]:

$$G_{\text{cr}} = 0.5\frac{P^2 d\eta}{dl}, \tag{1}$$

where G_{cr} is the elastic energy release rate in crack growth, P is the applied force, $\eta = \lambda/P$ is the pliability of the specimen (the reciprocal of specimen stiffness $M = P/\lambda$), λ is the applied load point displacements under elastic deformation of the specimen, and dl is the differential of the crack length. It follows from Eq. (1) that the elastic energy per new unit surface area of the crack, as it moves by a distance dl in a specimen whose thickness is a, can be written as

$$\gamma_{cr} = \frac{P^2 d\eta}{2a \cdot dl} = \frac{P^2 d\eta}{dS}, \tag{2}$$

where $dS = 2adl$ is the differential of the crack surface area. Hereinafter γ_{cr} will be referred to as the specific fracture energy.

The following formula is valid for a specimen shaped as a double-cantilever beam with a narrow rectilinear notch [8 and 10]:

$$\gamma_{cr} = \frac{12P^2 l^2}{Ea^2 b^3}. \tag{3}$$

The calculations accounting for chevron notch geometry allowed for derivation of an equation for a chevron-notched specimen:

$$\gamma_c = \frac{12P^2 l^2}{Ea^2 b^3} T, \tag{4}$$

where coefficient T is expressed as

$$T = \left[2 + \frac{a}{l_0}\cot\frac{\alpha}{2}\right]^2 \frac{k^{-1}}{4\Delta l}\cot\frac{\alpha}{2}\left(1 - \frac{l}{3}k^{-1}\frac{dk}{dl}\right). \tag{5}$$

Here parameter k is

$$k = \frac{2\Delta l}{a}\tan\frac{\alpha}{2}\left[2 + \frac{a}{l_0}\cot\frac{\alpha}{2}\right]^2 + \frac{l}{l_0}\left(1 - \frac{2\Delta l}{a}\tan\frac{\alpha}{2}\right)\left[4 + \frac{a}{l_0}\cot\frac{\alpha}{2} + \frac{2\Delta l}{l_0}\right] \tag{6}$$

and, accordingly,

$$\frac{dk}{dl} = \frac{2}{a}\tan\frac{\alpha}{2}\left[2 + \frac{a}{l_0}\cot\frac{\alpha}{2}\right]^2 + \frac{2l}{l_0^2}\left(1 - \frac{2\Delta l}{a}\tan\frac{\alpha}{2}\right) + \left[4 + \frac{a}{l_0}\cot\frac{\alpha}{2} + \frac{2\Delta l}{l_0}\right]\left(\frac{1}{l_0}\left(1 - \frac{2\Delta l}{a}\tan\frac{\alpha}{2}\right) - \frac{2l}{l_0 a}\tan\frac{\alpha}{2}\right), \tag{7}$$

where Δl is the crack growth increment and $l = l_0 + \Delta l$ is the crack length.

For a specimen treated as a symmetric double-cantilever beam, the following formula was derived for deflection of each cantilever, using methods of theory of elasticity:

$$\lambda^e = \frac{8P}{Eak}\left(\frac{l}{b}\right)^3\left[2 + \frac{a}{l_0}\cot\frac{\alpha}{2}\right]^2. \tag{8}$$

The equations derived here, unlike the standard relations from [2–5], incorporate no empirical constants. All the necessary characteristics can be obtained from experiment.

RESULTS

Figure 2 presents typical load-notch opening diagrams for the TV6 alloy in the CC (*a*) and UFG states (*b*) obtained in testing small-sized chevron-notched specimens. For the CC structure, crack nucleation occurs at the apex of

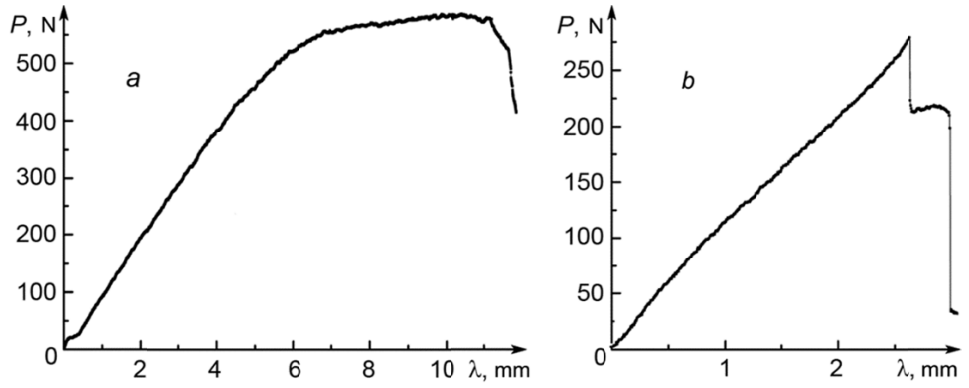

Fig. 2. Load-notch opening diagrams for the titanium alloy under study in the CC (*a*) and UFG states (*b*).

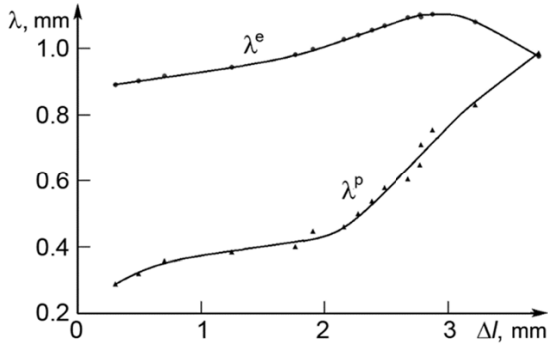

Fig. 3. Dependence of λ^e and λ^p on the increment in the crack length, *l*.

the chevron notch well before maximum loading P_{max} is attained. Until the applied stress is reduced, there is a long stage of stable crack growth with slightly varying external load. A different situation is observed in the case of the UFG material characterized by maximum loading [4] that determines the instant of crack nucleation at the apex of the chevron notch. The "plateau" in the *P*-λ curve corresponds to stable crack growth.

A comparison of the diagrams has revealed that SPD reduces the resistance of the material and gives rise to crack nucleation and growth. The calculation by Eq. (1) does show that the specific fracture energies of the VT6 alloy in the two states are essentially different from one another. The maximum fracture energies for the CC and UFG alloy structure are (44.3 ± 2.0) and (5.8 ± 1.0) kJ/m^2, respectively.

The calculations indicate that the double-cantilever beam deflection λ found experimentally is always larger than deflection λ^e caused by the release of the elastic energy as crack growth takes place (see Eq. (8)). Further contribution $\lambda^p = \lambda - \lambda^e$ not associated with variations in the crack length and hence with variations in the pliability of the specimen is especially pronounced in plastic materials. Figure 3 illustrates the dependence of λ^e and λ^p on the increment in crack length Δ*l* for the titanium alloy in the CC state. Contribution λ^p early in the crack growth is seen to exist and account for one third of the notch opening. This contribution is further increased and becomes comparable to the elastic deflection of the specimen at the instant of fracture ($\lambda^p/\lambda^e \approx 1$). In the UFG material, $\lambda^p/\lambda^e \leq 0.55$, i.e. the contribution of plastic deformation λ^p not associated with formation of a new crack surface is rather significant as well. This is evidence for the presence of a large plastic deformation zone in front of the crack tip. Because of this, the stress distribution in the UFG material differs essentially from that found in the elastic medium with a Griffith crack [6]. Consequently, K_{Ic} has no physical meaning.

Further information is acquired from surface fracture patterns obtained by SEM. Bright bands of porous fibrous structure indicative of SPD are seen on the fracture surface of the UFG alloy under study (Fig. 4). Fine structure of

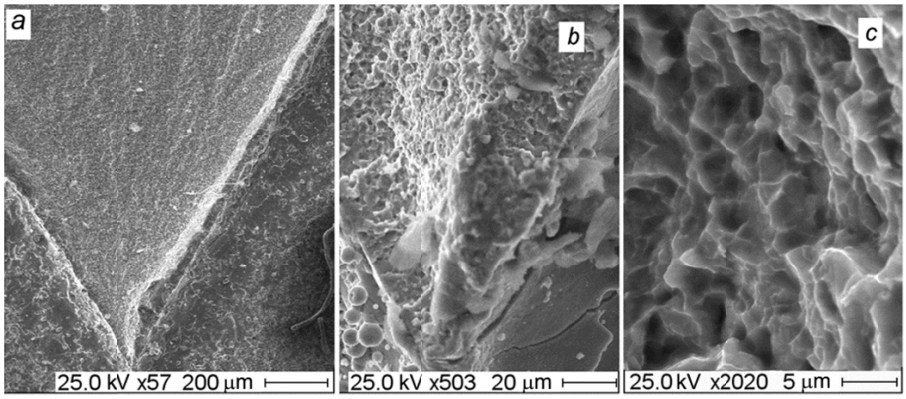

Fig. 4. Structure of plastic deformation bands on the fracture surface of the UFG alloy under study.

the plastic deformation bands on the fracture surface of the alloy exhibits high pore concentration and specimen fragmentation between pores (Fig. 4*b* and *c*). Foam-like band structure is evidence for an essential role of the deformation rotation modes in crack nucleation and growth in UFG materials. The crack is initiated at the apex of the chevron notch upon considerable local plastic deformation accompanied by local structural-phase decomposition of the original crystal structure [11 and 12]. The spacing between the bright bands is indicative of unstable crack growth.

SUMMARY

The specific fracture energy for stable crack growth in a VT6 alloy (Ti-6.46Al-3.84V) in the coarse-crystalline (γ_{cr} = (44.3 ± 2.0) kJ/m^2) and ultrafine-grained states (γ_{cr} = (5.8 ± 1.0) kJ/m^2) was estimated from testing small-sized chevron-notched specimens. Fractographic patterns of the fracture surface of the alloy were examined by scanning electron microscopy. The double-cantilever beam deflection was shown to contain a part not associated with variations in the pliability of the specimen with crack growth, i.e. with the work done by an external force to initiate a new fracture surface in the material.

According to concepts of physical mesomechanics, crack nucleation and growth result from two-phase decomposition of a strongly non-equilibrium material one phase of which is pores and discontinuities. Effects of this type occur in local hydrostatic tension zones characterized by an increased molar volume and near-zero Gibbs potential. The UFG material is from the outset in a strongly non-equilibrium state with an increased average molar volume. On the other hand, the boundary loading conditions provide a stressed state with a high level of normal tensile stresses at the apex of the chevron notch, which favors further increase in the molar volume and structural decomposition of the material. These factors are responsible for a reduction in the crack resistance of the alloy subjected to severe plastic deformation.

The band structure revealed on the fracture surface at the running crack arrest points cannot be realized by mechanisms involved in crystallographic shearing along densely packed lattice planes. This is evidence for an essential role of rotation deformation modes in crack nucleation and growth on different structural scales of the material.

The work is supported by Russian Foundation of Basic Research (Project No. 13-08-01404).

REFERENCES

1. ASTM Designation E 399-09: Standard Test Method for Linear-Elastic Plane-Strain Fracture Toughness K_{Ic} of Metallic Materials, PA, USA: West Conshohocken, 2009.
2. R. Sarkar and K. K. Ray, Fatigue Fracture Eng. Mater. Struct., **31**, No. 5, 340–345 (2008).

3. L. A. Alcaraz-Caracheo, J. Terán-Guillén, F. J. Carrión-Viramonte, and M. Martínez-Madrid, Científica, **16**, No. 3, 135–143 (2012).
4. T. J. Grant, L. Weber, and A. Mortensen, Eng. Fracture Mech., No. 67, 263–276 (2000).
5. C. T. Wang and R. M. Pillar, J. Mater. Sci., No. 24, 2391–2400 (1989).
6. E. E. Deryugin and G. V. Lasko, J. Appl. Mech. Tech. Phys., **39**, No. 6, 934–962 (1998).
7. R. W. Hertzberg, Deformation and Fracture Mechanics of Engineering Materials, 3rd ed., Wiley, N.Y. (1989).
8. Yu. G. Matvienko, Models and Criteria of Fracture Mechanics [in Russian], Fizmatlit, Moscow (2006).
9. V. A. Vinokurov, I. V. Ratochka, E. V. Naydenkin, *et al.,* Rf Patent № 2388566 (10 May, 2010).
10. D. Broek, Fundamentals of Fracture Mechanics [in Russian], Vysshaya Shkola, Moscow (1980).
11. V. E. Panin, V. E. Egorushkin, and A. V. Panin, Phys. Mesomech., **15,** Nos. 1–2, 1–12 (2012).
12. V. E. Panin, V. E. Egorushkin, L. S. Derevyagina, and E. E. Deryugin, Phys. Mesomech., **16**, No. 3, 183–190 (2013).